Central European Journal of Energetic Materials
ISSN 1733-7178; e-ISSN 2353-1843

Cent. Eur. J. Energ. Mater., 2016, *13*(4), 916-926; DOI: 10.22211/cejem/65826

The Microstructural Evolution in HMX Based Plastic-bonded Explosive During Heating and Cooling Process: an *in situ* Small-angle Scattering Study

Guanyun YAN,[1*] Qiang TIAN,[1] Jiahui LIU,[2] Zhijian FAN,[1] Guangai SUN,[1] Changsheng ZHANG,[1] Yunlong WANG,[1] Bo CHEN,[1] Jian GONG,[1] Xiaoqing ZHOU,[2] Zhanfeng YANG,[2] Fude NIE,[2] Jingming LI,[2] Xiuhong LI [3]

[1] *Key Laboratory of Neutron Physics and Institute of Nuclear Physics and Chemistry, China Academy of Engineering Physics, Mianyang 621999, China*
[2] *Institute of Chemical Materials, China Academy of Engineering Physics, Mianyang 621999, China*
[3] *Institute of Shanghai Apply Physics, Chinese Academy of Science, Shanghai 201800, China*
[*] *E-mail: yanguany@126.com*

Abstract: The thermal damage in octahydro-1,3,5,7-tetranitro-1,3,5,7-tetrazocine (HMX) based plastic-bonded explosive (PBX) was investigated using *in situ* small-angle neutron and X-ray scattering techniques. The microstructural evolution was quantitatively characterized by the model fitting parameters of total interfacial surface area (S_v) and void volume distribution. The S_v of HMX-PBX decreased markedly above 100 °C, indicating the movement of binder into the voids. After subsequent cooling to room temperature, the scattering intensity increased significantly with increasing storage time, and a new population of voids with average diameter of 20 nm was observed, accompanied by the gradual phase transition of HMX from δ- to β-phase. The experimental results implied that serious damage within the HMX-PBX was developed during storage after heating.

Keywords: SANS, SAXS, HMX-PBX, thermal damages, phase transition

1 Introduction

Octahydro-1,3,5,7-tetranitro-1,3,5,7-tetrazocine (HMX) based plastic bonded explosives (PBXs) have extensive industrial and military applications. When HMX-PBXs are subjected to unexpected heat, thermal effects can result in phase transitions, thermal expansion and decomposition, which are associated with the generation of pores and cracks. The resulting damaged HMX-PBXs will be more sensitive to shock or impact initiation because of the increase of potential "hot spots" induced by defects and the more sensitive δ-phase HMX [1-4]. Therefore, characterizing and understanding thermal effects are important for predicting the performance of HMX-PBXs in accident scenarios.

HMX has a monoclinic β-phase and converts to a hexagonal δ-phase when heated to 160-180 °C [5]. The phase transition leads to obvious changes in crystal morphology and density, which are likely to create new populations of defects. The technique of small-angle X-ray/neutron scattering (SAXS/SANS) is ideally suited for investigating nano-scale defects in explosives and can provide quantitative information of void-size distribution and specific surface area [6-8]. Using SAXS, Mang *et al.* [9] showed that large pores and cracks developed in HMX at 180 °C, associated with the β→δ phase transition. Peterson *et al.* [10] found that a population of smaller voids with a mean radius of 11 nm developed at 176 °C in thermally-treated PBX 9501 (95% HMX, 2.5% Estane, and 2.5% nitroplasticizer). In our previous research, the SAXS technique was used to study the effects of HMX crystal particle size on the thermal damage of HMX-PBX as well as the evolution of voids in hexanitrohexaazaisowurtzitane (CL-20) during phase transition and decomposition [11, 12].

It has been reported that δ-phase HMX can partially revert back to the β-phase at room temperature (RT) over a period of several days [5]. Moreover, the phase transition behaviour of pure HMX is quite different to that of HMX incorporated into PBXs. For example, Saw and Tarver [13] reported that, in the presence of the PBX 9501 binder, the δ-phase of HMX readily converts back to the β-phase during cooling, but no reverse phase transition is observed in the absence of the polymer binder. It can be expected that the reverse phase transition behaviour of HMX could also influence the microstructure of an HMX-PBX. Thus, a remaining question is how the β→δ and δ→β phase transitions affect the new voids and other defects. It is of importance from both the basic and applied viewpoints to determine the microstructural evolution of HMX-PBX induced by heating and subsequent cooling and storage.

In a recent work, Willey *et al.* [14] studied the microstructural evolution of HMX-PBXs during heating by means of *in situ* ultra SAXS. They found that

the microstructure of the samples dramatically changed with the β→δ phase transition, and the void volume increased when the samples were cooled to RT. However, up to now, there is little information related to the after-heating storage behaviours of HMX-based PBXs. In the study reported here, an HMX-PBX sample was thermally treated to induce the β→δ HMX phase transition. The microstructural evolution during the heating and after-heating storage process was also investigated by the *in situ* SANS and SAXS techniques. Our findings therefore provide additional information for understanding the thermal effects on HMX-PBXs.

2 Materials and Methods

HMX-PBX disks 10 mm in diameter and 1 mm in thickness were prepared by compression molding at RT. The samples had an average density of 1.72 g/cm^3 and consisted of 95% HMX (with a mean particle size of 40 μm) and 5% fluorine rubber (F_{2314}, Zhonghao Chenguang Research Institute of Chemical Industry, China) only (no other additives). SAXS measurements were conducted at BL16B1 of the Shanghai Synchrotron Radiation Facility [15] with X-ray photons energy of 10 keV (corresponding to a wavelength of 0.124 nm) to monitor the microstructural evolution of the HMX-PBX during heating. The detector was placed at a distance of 2075 mm from the sample, covering a q-interval of 0.1-2 nm^{-1}. A Linkam stage (THMS600) was used to heat the sample and control the temperature. The HMX-PBX was first heated to 140 °C at a heating rate of 4 K/min, and then heated to 200 °C at a heating rate of 1 K/min. The sample was then kept at 200 °C for 60 min to ensure a complete β→δ phase transition. After storage at RT for 30 days, the HMX-PBX was investigated again using SAXS to check the microstructural evolution.

The SANS experiments were performed on the small-angle neutron scattering diffractometer at the Institute of Nuclear Physics and Chemistry, China Academy of Engineering Physics. A multiblade mechanical velocity selector was used to make a monochromatic beam with a mean wavelength of 0.48 nm and 0.11 FWHM. A ^{3}He gas filled multiwire detector with a 64 × 64 cm^2 sensitive area was placed at a distance of 7.1 m from the sample, to cover the q-range of 0.06-0.6 nm^{-1}. The sample was heated to 185 °C at 5 K/min, the temperature was then held constant at 185 °C for 60 min to induce complete β→δ phase transition, and finally cooled to RT in 30 min. The SANS measurements were carried out at 17 min intervals during the subsequent after-heating storage at RT. The recorded 2D patterns were converted into one-dimensional profiles using the

MySAS package [16]. The data reduction corrects the raw measured data for the contributions of the empty cell and background, thickness, and transmission. The absolute intensities of the SAXS and SANS data were calculated using a 1 mm thick water sample and direct beam methods, respectively.

Scattering is caused by fluctuations in the electron density or scattering length density $\rho(r)$ and reflects the microstructure of the materials. The scattering intensity $I(q)$ is measured as a function of scattering vector $q = 4\pi \cdot \sin\theta/\lambda$, where λ is the wavelength of the incident radiation, and θ is half of the scattering angle. Porous or fine granulated materials which have smooth surfaces or interfaces exhibit characteristic scattering curves with a q^{-4} decay behaviour (*i.e.*, $I(q)$ is proportional to q^{-4} in logarithmic coordinates). Porod's law was employed to analyze the data, which can be expressed as [17]:

$$I = \frac{2\pi\Delta\rho^2(S/V)}{q^4} + I_b \tag{1}$$

where $\Delta\rho = \rho_s - \rho_{matrix}$ is the contrast between the matrix (ρ_{matrix}) and the scattering particles (ρ_s) (which are assumed here to be empty voids), and I_b is a constant which accounts for the background. S/V is the interfacial surface area per unit volume (S_v). Furthermore, $I(q)$, for a polydisperse system of non-interacting particles dispersed in a uniform medium, can be expressed as [18]:

$$I(q) = \Delta\rho^2 \int_0^\infty NP(D)V^2(D)F^2(q,D)dD \tag{2}$$

where D is the diameter of the particle, $F^2(q, D)$ is the form factor, $V(D)$ is the volume of the particle, N is the total number of minority phase particles per unit volume, and $P(D)$ is the probability of having a minority phase particle of size D. The neutron scattering length density (ρ) can be calculated by [19]:

$$\rho = \frac{\sum_{i=1}^{n} b_{c_i}}{V_m} \tag{3}$$

where b_{c_i} is the bound coherent scattering length of the ith out of n atoms in a molecule with molecular volume V_m. The scattering length densities of β-phase HMX, δ-phase HMX, and F_{2314} are 4.50×10^{10} cm^{-2}, 4.22×10^{10} cm^{-2}, and 3.95×10^{10} cm^{-2}, respectively. The scattering length density of voids in HMX-PBX is equal to 0 cm^{-2}. Hence, the studied multi-phase system can be simplified as a two-phase system composed of voids with different sizes dispersed in a homogeneous matrix. The volume fraction of these voids, calculated using

the "Irena" package (which uses a maximum entropy algorithm) can be expressed as [18]:

$$V_{total} = \int_0^\infty NP(D)V(D)dD \tag{4}$$

The crystal structures of the thermally treated HMX-PBX were further investigated using a D8 ADVANCE X-ray diffractometer (XRD) equipped with Cu K_a radiation. The same batch of HMX-PBX was heated in an aging chamber at 185 °C for 60 min, and then immediately transferred to the XRD instruments.

3 Results and Discussion

The SAXS data of HMX-PBX upon heating at RT, 100, 180, and 200 °C are shown in Figure 1. All of the scattering curves have a similar shape and the scattering intensity decreases with temperature, which implies a loss of scatterers within the sample. The slope of the scattering curves was found to be approximately equal to 4, so Porod's law was applied to determine the S_v of HMX-PBX. The S_v and the temperature as a function of the heating time are shown in Figure 2. The S_v decreases slightly until 100 °C, and then, decreases dramatically by 60% at 200 °C.

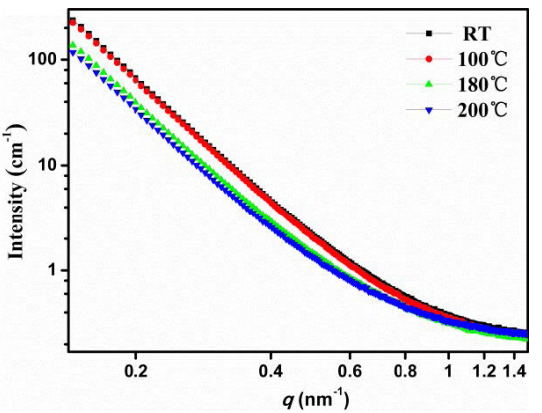

Figure 1. SAXS curves of HMX-PBX heated at RT, 100 °C, 180 °C, and 200 °C.

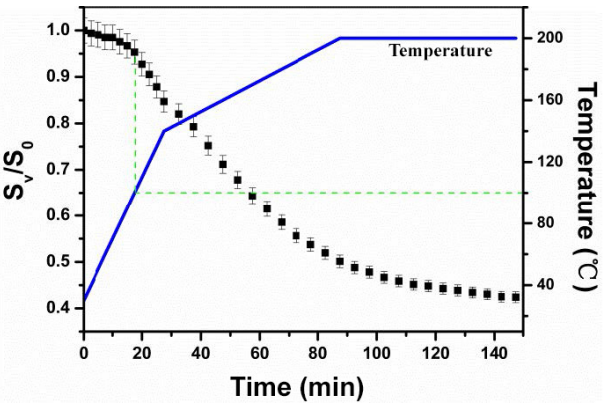

Figure 2. Interfacial surface area (normalized to the original state) of HMX-PBX and temperature as a function of heating time.

The scattering intensity of the thermally treated HMX-PBX increases obviously after storage at RT for 30 days (Figure 3). A shoulder appearing at a q range of 0.1-0.4 nm^{-1} is observed, which indicates a new population of defects developing at RT. To further study the detailed evolution of these defects, SANS measurements were carried out during the after-heating storage process and the results are presented in Figure 4. The scattering intensity can be seen to increase gradually with the storage time, and the shoulder becomes increasingly pronounced with storage times up to 85 min. Herein, we assume the new defects are spherical voids and apply the maximum entropy method as an approximate model to fit the SANS data.

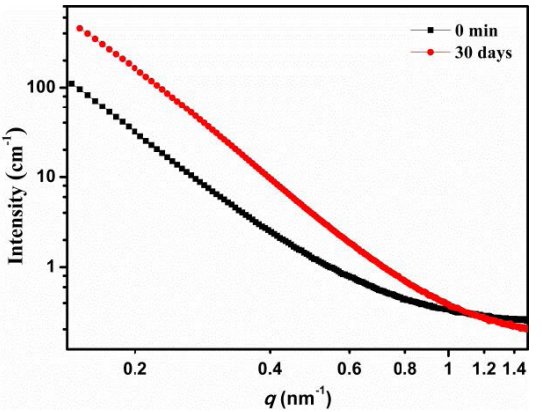

Figure 3. SAXS results of the thermally treated HMX-PBX stored at RT for 0 and 30 days.

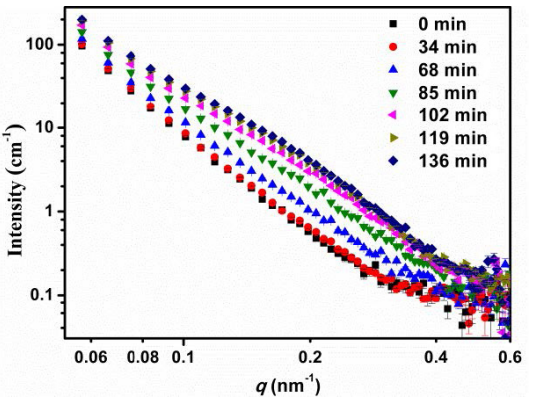

Figure 4. SANS curves of the HMX-PBX during the after heating storage at RT.

The void volume distributions analyzed using the maximum entropy method are shown in Figure 5. A distinct increase of voids with sizes between 15 and 35 nm occurred during storage. The volume fraction showed a steep increase until 170 min, and then increased slowly from 170 min to 680 min, as shown in Figure 6. The void volume fraction (from 1 nm to 110 nm) of the sample increased to 0.2003% at 680 min when the SANS measurements ended.

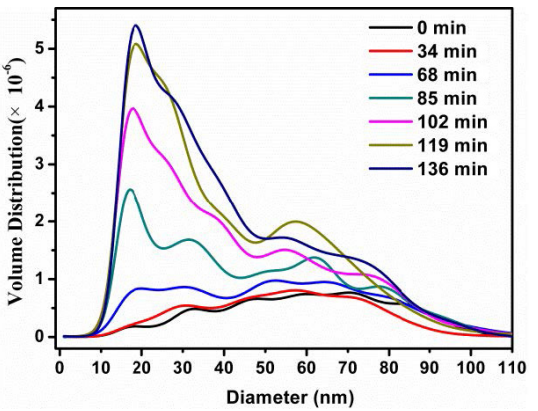

Figure 5. Void volume distribution of thermally treated HMX-PBX during the storage.

The XRD patterns (Figure 7) acquired for the raw sample and immediately after heating at 185 °C can be indexed to β- and δ-phase HMX, respectively. The δ- and β-phases of HMX coexisted within the sample kept at RT for 1-3 hours.

The degree of transition from the δ- to the β-phase (as indicated by the increased intensity of the β phase peak at 20.6°) exhibited a significant increase 30 days later. These results demonstrate the β→δ phase transition during after-heating storage, in agreement with previous studies [5, 13].

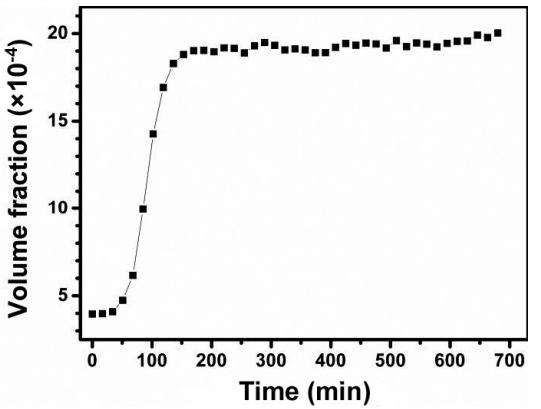

Figure 6. Normalized volume fraction of thermal treated HMX-PBX as a function of storage time at room temperature (30 °C).

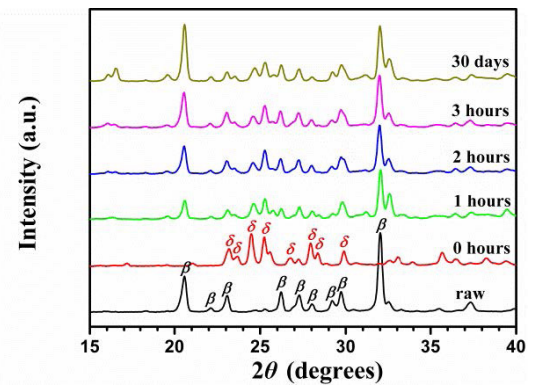

Figure 7. XRD patterns of the HMX-PBX measured before and after heating.

Most of the initial voids in the HMX-PBX studied came from the synthesis and manufacture processes. The S_v can reflect the microstructural changes of HMX-PBX during the heating process. Upon thermal loading, the initial voids could be filled by the binder because of the decrease in the binder viscosity [20, 21]. The melt temperature of the F_{2314} binder is about 97 °C [22], so the dramatic decrease of the S_v at temperatures higher than 100 °C is mainly attributed to the filling of the initial voids by the F_{2314} binder.

The densities of the β- and δ-phases of HMX are 1.897 g/cm^3 and 1.76 g/cm^3, respectively. The conversion of β- to δ-phase HMX during the heating process is accompanied by a change in crystal morphology and about a 7% volume expansion, which may result in new cracks and voids. In this study, the expected increase of the interfacial surface area induced by the β→δ phase transition is not observed, a difference to Willey's results [14]. The difference may be attributed to the discrepancy in the initial structure and chemical composition of the samples. The HMX-PBXs used in this study have a lower density of 1.72 g/cm^3 than that of LX 10 (1.82 g/cm^3) and PBX 9501 (1.87 g/cm^3). The initial porosity in our samples is 5% higher, so the filling of the initial voids by the F_{2314} binder will be more predominant. Therefore, the increase of cracks and voids induced by β→δ phase transition upon heating appears to be suppressed and compensated for the filling effects of the binder.

During the after-heating storage, the rate of δ→β phase transition (accompanied by a decrease in volume) becomes quite slow at room temperature, resulting in tensile stresses in the HMX-PBX. If the stress exceeds the fracture limits, cracks and voids will initiate at local stress concentration zones (such as dislocations, grains, and interfaces between HMX crystal and binders) thereby acting as a stress relaxation mechanism. These defects may propagate due to the tensile stresses induced by the gradual transition of HMX from the δ- to the β-phase. So there is a marked increase of the voids during after-heating storage as shown in the experimental results.

In the SAXS experiments, the defect evolution in thermally treated HMX-PBX was interpreted in terms of the β→δ phase transition of HMX [10, 11, 14]. In this study, our findings show that significant damage of the thermally treated (above the HMX phase transition temperature) HMX-PBX develops during the after-heating storage process. This damage is time dependent and accompanied by the much slower δ→β phase transition of HMX.

4 Conclusions

In situ SANS and SAXS measurements were carried out to characterize the thermal damage in HMX-based PBXs. The S_v of HMX-PBXs significantly decreased above 100 °C, suggesting that the initial voids in the HMX-PBXs were infilled by the melting binder. After subsequent cooling and storage at RT, a new population of voids with sizes between 15 nm and 35 nm was developed in the HMX-PBX during the δ→β phase transition of HMX. Our findings show for the first time that significant damage of the HMX-PBX thermally treated

above the phase transition temperature occurs during the after-heating storage process. The results are useful for understanding and predicting the performance of thermally damaged HMX-PBX in accident scenarios.

Acknowledgments
This work has been supported by the National Natural Science Foundation of China under grant Nos. 11205137, 11302199 and U1330202.

References

[1] Hsu P.C., DeHaven M., McClelland M., Tarver C., Chidester S., Maienschein J., Characterization of Damaged Materials, *13th Int. Detonation Symposium*, Norfolk, Virginia, July 23-28, **2006**, 617.
[2] Asay B.W., Henson B.F., Smilowitz L.B., Dickson P., On the Difference in Impact Sensitivity of Beta and Delta HMX, *J. Energ. Mater.*, **2003**, *21*, 223-235.
[3] Tringe J., Kercher J., Springer H., Glascoe E., Levie H., Hsu P., Willey T., Molitoris J., Numerical and Experimental Study of Thermal Explosions in LX-10 and PBX 9501: Influence of Thermal Damage on Deflagration Processes, *J. Appl. Phys.*, **2013**, *114*, 043504.
[4] Menikoff R., Sewell T.D., Constituent Properties of HMX Needed for Mesoscale Simulations, *Combust. Theor. Model.*, **2002**, *6*, 103-125.
[5] Xue C., Sun J., Kang B., Liu Y., Liu X., Song G., Xue Q., The β-δ-Phase Transition and Thermal Expansion of Octahydro-1,3,5,7-tetranitro-1,3,5,7-tetrazocine, *Propellants Explos. Pyrotech.*, **2010**, *35*, 333-338.
[6] Stoltz C.A., Mason B.P., Hooper J., Neutron Scattering Study of Internal Void Structure in RDX, *J. Appl. Phys.*, **2010**, *107*, 103527.
[7] Mang J.T., Hjelm R.P., Small-Angle Neutron Scattering and Contrast Variation Measurement of the Interfacial Surface Area in PBX 9501 as a Function of Pressing Intensity, *Propellants Explos. Pyrotech.*, **2011**, *36*, 439-445.
[8] Mang J.T., Hjelm R.P., Fractal Networks of Inter-Granular Voids in Pressed TATB, *Propellants Explos. Pyrotech.*, **2013**, *38*, 831-840.
[9] Mang J., Skidmore C., Son S., Hjelm R., Rieker T., An Optical Microscopy and Small-angle Scattering Study of Porosity in Thermally Treated PBX 9501, *AIP Conf. Proc.*, **2002**, *620*, 833-836.
[10] Peterson P.D., Mang J.T., Asay B.W., Quantitative Analysis of Damage in an Octahydro-1,3,5,7-tetranitro-1,3,5,7-tetrazonic-based Composite Explosive Subjected to a Linear Thermal Gradient, *J. Appl. Phys.*, **2005**, *97*, 093507.
[11] Yan G.Y., Tian Q., Liu J.H., Chen B., Sun G.A., Huang M., Li X.H., Small-angle X-ray Analysis of the Effect of Grain Size on the Thermal Damage of Octahydro-1,3,5,7-tetranitro-1,3,5,7-tetrazocine-based Plastic-bounded Expolsives, *Chin. Phys. B.*, **2014**, *23*, 076101.

[12] Tian Q., Yan G.Y., Sun G.A., Huang C., Xie L., Chen B., Huang M., Li H.Z., Liu X., Wang J., Thermally Induced Damage in Hexanitrohexaazaisowurtzitane, *Cent. Eur. J. Energ. Mater.*, **2013**, *10*(3), 359-369.
[13] Saw C.K., Tarver C.M., Binder/HMX Interaction in PBX9501 at Elevated Temperatures, *AIP Conf. Proc.*, **2004**, *706*, 1029-1032.
[14] Willey T.M., Lauderbach L., Gagliardi F., van Buuren T., Glascoe E.A., Tringe J.W., Lee J.R., Springer H.K., Ilavsky J., Mesoscale Evolution of Voids and Microstructural Changes in HMX-based Explosives During Heating Through the β→δ Phase Transition, *J. Appl. Phys.*, **2015**, *118*, 055901.
[15] Jiang M., Yang X., Xu H., Zhao Z., Ding H., Shanghai Synchrotron Radiation Facility, *Chin. Sci. Bull.*, **2009**, *54*, 4171-4181.
[16] Huang Ch., Xia Q., Yan G., Sun G., Chen B., A New Package: MySAS for Small Angle Scattering Data Analysis, *Nuc. Sci. Tech.*, **2010**, *21*, 325-329.
[17] Glatter O., Kratky O., *Small Angle X-ray Scattering*, Academic Press London, **1982**, Vol. 66.
[18] Ilavsky J., Jemian P.R., Irena: Tool Suite for Modeling and Analysis of Small-angle Scattering, *J. Appl. Crystallogr.*, **2009**, *42*, 347-353.
[19] Koester L., Rauch H., Seymann E., Neutron Scattering Lengths: a Survey of Experimental Data and Methods, *At. Data Nucl. Data Tables*, **1991**, *49*, 65.
[20] Levitas V.I., Henson B.F., Smilowitz L.B., Asay B.W., Solid-solid Phase Transformation via Virtual Melting Significantly Below the Melting Temperature, *Phys. Rev. Lett.*, **2004**, *92*, 235702.
[21] Levitas V.I., Henson B.F., Smilowitz L.B., Zerkle D.K., Asay B.W., Coupled Phase Transformation, Chemical Decomposition, Deformation in Plastic-bonded Explosive: Models, *J. Appl. Phys.*, **2007**, *102*, 113502.
[22] Li J.L., Wang X.C., Sun J., Aging Effect of the Crystallization Behavior of VDF/CTFE, *Eng. Plast. Appl.* (in Chinese), **2007**, *4*, 015.